



## Thermochromic textile sensors for temperature measurements

Malwina Jaszczak-Kuligowska<sup>a,\*</sup>, Elżbieta Sasiadek-Andrzejczak<sup>a</sup>, Marta Safandowska<sup>b</sup>,  
Marek Kozicki<sup>a</sup>, Laura Florentino Madiedo<sup>c,d</sup>, Marcin Barburski<sup>e</sup>, David Ranz<sup>f</sup>,  
Reyes Mallada<sup>c,d</sup>

<sup>a</sup> Department of Mechanical Engineering, Informatics and Chemistry of Polymer Materials, Faculty of Materials Technologies and Textile Design, Lodz University of Technology, Żeromskiego 116, 90-543 Lodz, Poland

<sup>b</sup> Centre of Molecular and Macromolecular Studies, Polish Academy of Sciences, Sienkiewicza 112, 90-363 Lodz, Poland

<sup>c</sup> Instituto de Nanociencia y Materiales de Aragón (INMA), CSIC-Universidad de Zaragoza, Zaragoza 50009, Spain

<sup>d</sup> Chemical and Environmental Engineering Department, Universidad de Zaragoza 50018, Spain

<sup>e</sup> Institute of Architecture of Textiles, Faculty of Materials Technologies and Textile Design, Lodz University of Technology, Żeromskiego 116, 90-543 Lodz, Poland

<sup>f</sup> Department of Design and Manufacture Engineering, University of Zaragoza, María Luna 3, 50018 Zaragoza, Spain

### ARTICLE INFO

#### Keywords:

Thermochromic sensor  
Thermochromic pigment  
Temperature changes indicator  
Textile sensor  
Wool textile  
Screen printing

### ABSTRACT

This study presents woollen textiles printed with thermochromic pigments by the screen-printing method for use as new sensors for temperature measurements. The sensors demonstrate reversible colour changes due to temperature variations, which were measured using reflectance spectrophotometry. The beginning of thermal activation of the pigment is registered below 23 °C, the main action takes place in the range of 30–45 °C, and its complete discolouration occurs at 50 °C. The uniformity of the print and pigment distribution on the fabric surface was confirmed using scanning electron microscopy (SEM). Furthermore, a comprehensive chemical analysis of the commercially available thermochromic pigment was performed using elemental analysis, energy-dispersive X-ray spectroscopy (EDX), X-ray photoelectron spectroscopy (XPS), X-ray diffraction (XRD), nuclear magnetic resonance spectroscopy (NMR), Fourier transform infrared spectroscopy (FTIR), and differential scanning calorimetry (DSC) techniques. Based on this research, it was determined that the pigment has a spirobenzoxadiazine core structure with amide and imine functional groups. The paper also discusses potential applications of the developed sensors, highlighting their promise as temperature sensors, as well as security, marking, and decorative elements, usable independently or as a part of a composite. Additionally, their potential for two-dimensional temperature distribution measurements was indicated.

### 1. Introduction

Thermochromic materials exhibit a colour change in response to temperature variations. This alteration may involve a transition between two distinct colours, from a colourless to a coloured form, or from a coloured to a colourless form. The colour change may be reversible or irreversible and can occur gradually or violently at a specific temperature threshold [1–4].

In thermochromic materials, thermochromic pigments or dyes are responsible for the colour change. The terms *dye* and *pigment* are often used interchangeably, but they differ in many features, mainly in (i) their chemical composition, (ii) behaviour in medium, (iii) the

mechanism of colour change, (iv) stability, and (v) their possible applications. These differences influence the choice between using thermochromic pigments or dyes depending on the desired properties and applications. Thermochromic pigments are usually organic or inorganic compounds from the groups of inorganic salts, inorganic oxides or spiro compounds. They are insoluble in the medium in which they are used, and they are dispersed in it as particles. They do not undergo chemical reactions with the surrounding medium or substrate. The mechanism of their colour change involves selective absorption and/or scattering of light. Their colour properties depend on their chemical structure and physical characteristics of their particles, and their colour change may be reversible or irreversible. Furthermore, thermochromic pigments

\* Corresponding author.

E-mail addresses: [malwina.jaszczak@p.lodz.pl](mailto:malwina.jaszczak@p.lodz.pl) (M. Jaszczak-Kuligowska), [elzbieta.sasiadek@p.lodz.pl](mailto:elzbieta.sasiadek@p.lodz.pl) (E. Sasiadek-Andrzejczak), [marta.safandowska@cbmm.lodz.pl](mailto:marta.safandowska@cbmm.lodz.pl) (M. Safandowska), [marek.kozicki@p.lodz.pl](mailto:marek.kozicki@p.lodz.pl) (M. Kozicki), [lflorentino@unizar.es](mailto:lflorentino@unizar.es) (L.F. Madiedo), [marcin.barburski@p.lodz.pl](mailto:marcin.barburski@p.lodz.pl) (M. Barburski), [dranz@unizar.es](mailto:dranz@unizar.es) (D. Ranz), [rmallada@unizar.es](mailto:rmallada@unizar.es) (R. Mallada).

<https://doi.org/10.1016/j.measurement.2025.118698>

Received 14 May 2025; Received in revised form 10 July 2025; Accepted 11 August 2025

Available online 13 August 2025

0263-2241/© 2025 The Authors. Published by Elsevier Ltd. This is an open access article under the CC BY license (<http://creativecommons.org/licenses/by/4.0/>).

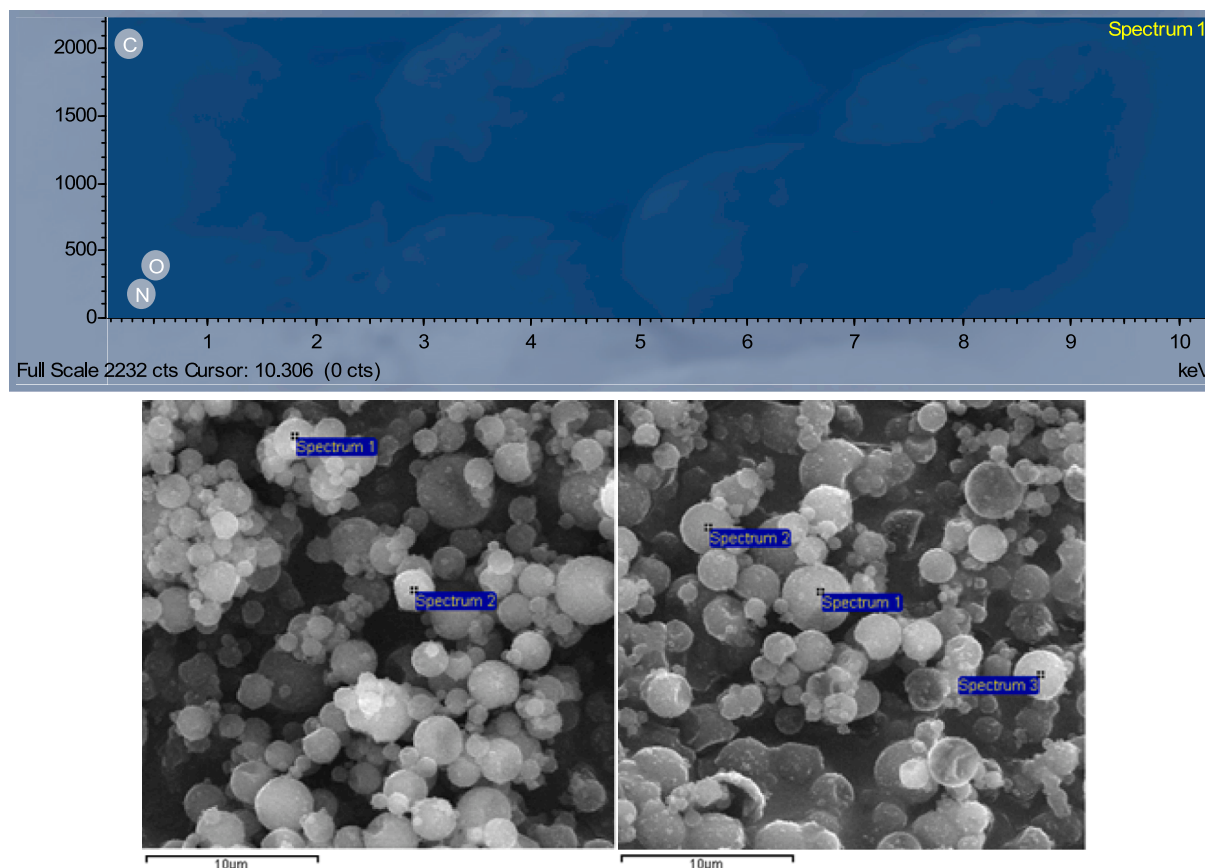


Fig. 1. EDX spectrum of the thermochromic pigment (above) with SEM images showing where the EDX analyses were performed (below).

Table 1

EDX analysis weight % results of thermochromic pigment.

	C	N	O
Spectrum 1 (wt. %)	61.41	23.64	14.95
Spectrum 2 (wt. %)	61.54	23.99	14.47
Spectrum 3 (wt. %)	64.31	18.58	17.11
Spectrum 4 (wt. %)	64.25	19.56	16.19
Spectrum 5 (wt. %)	62.01	19.66	18.33
Mean (wt. %)	63	21	16
Std. Dev.	1	3	2
Atomic ratio	11	3	2
Atomic %	68	19	13

generally exhibit high stability and resistance to factors such as light, heat, and chemical reagents, making them suitable for long-term use. For their application, pigments require attachment to the substrate by additional compounds, e.g., by the polymer in the paint in which they are dispersed. On the other hand, thermochromic dyes are predominantly organic compounds featuring a chromophore group (mainly leuco dyes). Unlike pigments, thermochromic dyes are soluble in the medium in which they are used and thus disperse at a molecular level. A key distinction is their capacity to undergo chemical reactions with the surrounding medium or substrate. Their colour change mechanism primarily relies on the selective absorption of light, and their colour properties are mainly determined by their chemical structure. The colour changes observed with dyes are typically irreversible. Regarding stability, thermochromic dyes are generally less permanent and light stable than pigments, and their exposure to UV radiation commonly leads to fading and degradation. For effective application, dyes must possess a specific affinity for the substrate onto which they are applied [2,5–10].

Thermochromic materials have been known since the 1970s. Their development significantly accelerated in the 21st century, with initial applications primarily focused on decorative elements and indicators that inform about temperature changes in textiles, packaging, and everyday products. Subsequently, thermochromic materials were developed for more advanced technological applications, such as anti-counterfeiting technology, drug delivery systems, the pharmaceutical industry, safety equipment, food and agriculture, military technology, energy-efficient construction, and aerospace [1,4,11–13]. For these applications, various types of temperature-sensitive sensors are used. To produce thermochromic materials, thermochromic dyes and pigments are often added to polymer solutions, which can then be used to produce thermochromic coatings [14–17], microcapsules [14,18,19], or fibres [14,20]. They are also incorporated into inks, paints, and printing pastes, which can be used to cover plastics, paper, or textile surfaces [14,21–24]. The existing literature does not fully exhaust the topic of developing markers and sensors for measuring temperature changes, hence, the idea of developing a new thermochromic sensor appeared. A part of this study was additionally dedicated to the chemical analysis of the thermochromic pigment used, which is an aspect often neglected in other published works. Commercially available thermochromic pigments typically lack detailed chemical composition information in both distributor datasheets and literature.

This study aimed to develop a thermochromic sensor on a textile substrate. For this purpose, a wool fabric was printed with a printing paste containing a thermochromic pigment using the screen-printing method. The selection of textile as the substrate ensures the flexibility of the sensor and the possibility of its use in numerous applications. To combine ecological aspects in line with the concept of sustainable development with innovative solutions, wool was chosen as the textile substrate due to its environmentally friendly and biodegradable nature. A reversible pigment was used as the thermochromic colourant, which

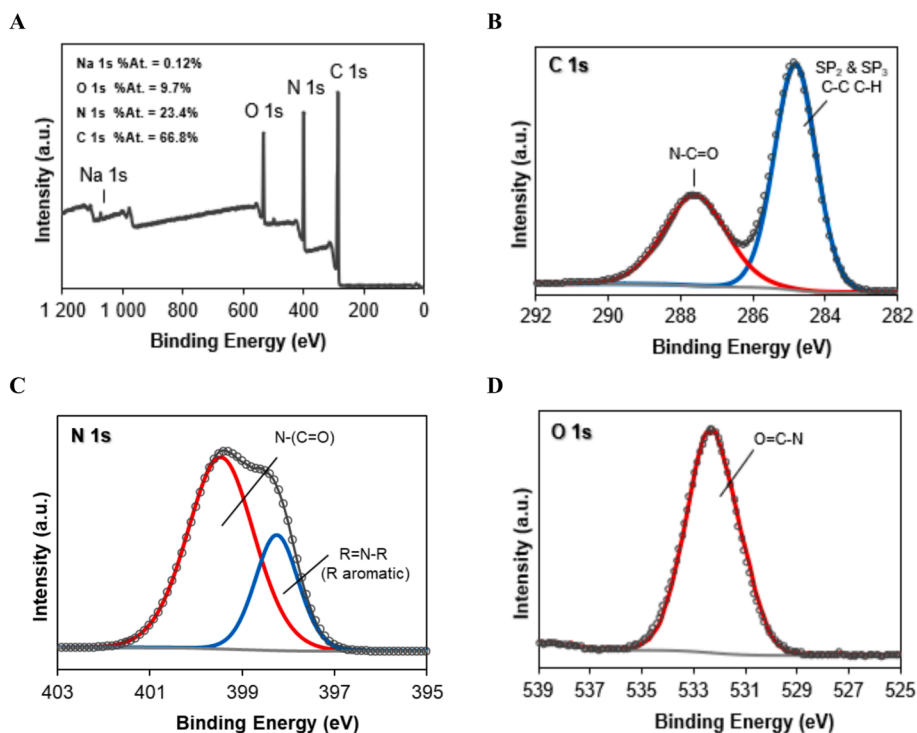


Fig. 2. XPS spectra of thermochromic pigments: broad scan (A), deconvoluted carbon 1s spectra (B), deconvoluted nitrogen 1s spectra (C), deconvoluted oxygen 1s spectrum (D).

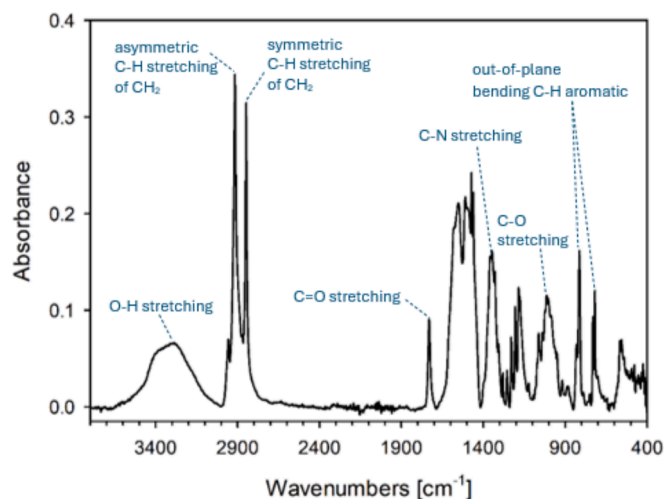


Fig. 3. Fourier transform infrared (FTIR) spectra of thermochromic pigment.

ensures high stability and resistance to light and chemical reagents, as well as enables multiple uses of the sensor. The screen-printing method was used for the production of the sensors, which is a simple, economical, and environmentally friendly approach due to the minimal consumption of printing paste. This research introduces a novel and original approach by creating a new temperature-sensitive sensor that is simultaneously (i) flexible, (ii) reversible, (iii) reusable, (iv) easy to produce, use, and read, (v) developed on an ecological, natural, and biodegradable textile substrate in the idea of sustainable development, (vi) manufactured by printing on fabric with only one active side to prevent potential skin allergies upon contact, and (vii) contains a thermochromic pigment that has been chemically characterised within this study. As part of this work, a comprehensive characterisation of the sensor was performed, including (i) its temperature response and stability

measurements using reflectance spectrophotometry, (ii) evaluation of print uniformity using RGB channel and scanning electron microscopy (SEM) analysis, (iii) chemical composition characterisation of the commercially available thermochromic pigment using the elemental analysis, as well as energy-dispersive X-ray spectroscopy (EDX), X-ray photoelectron spectroscopy (XPS), X-ray diffraction (XRD), nuclear magnetic resonance spectroscopy (NMR), and Fourier transform infrared spectroscopy (FTIR) techniques, and (iv) thermal analysis of the pigment using differential scanning calorimetry (DSC). Furthermore, the sensors were incorporated into composites, and their effect on temperature changes and the possibility of their use in such structures were assessed. Additionally, potential applications of the developed thermochromic sensors were presented, including their use as decorative elements, protective elements for textile products, temperature sensors on everyday accessories, sensors measuring temperature distribution in 2D, as well as parts of the composites for various applications, for example, drone casings.

## 2. Materials and methods

### 2.1. Scanning electron microscopy (SEM) with energy-dispersive X-ray spectroscopic (EDX) analysis

The morphology of the samples was analysed using a field-emission scanning electron microscope (SEM, FEI Inspect F50; Thermo Fisher Scientific, formerly FEI, Waltham, MA, USA) with a typical acceleration voltage of 10 kV. The samples were deposited on carbon conductive tape and metallised with palladium. The particle size was measured from these images using ImageJ software (National Institutes of Health and the Laboratory for Optical and Computational Instrumentation, LOCI, University of Wisconsin).

The compositional analysis was performed using Energy-Dispersive X-ray Spectroscopy (EDX) detector, at an accelerating voltage of 20 kV, and a working distance of approximately 10 mm. For the EDX analysis, the samples were coated with a carbon layer to ensure optimal signal detection.

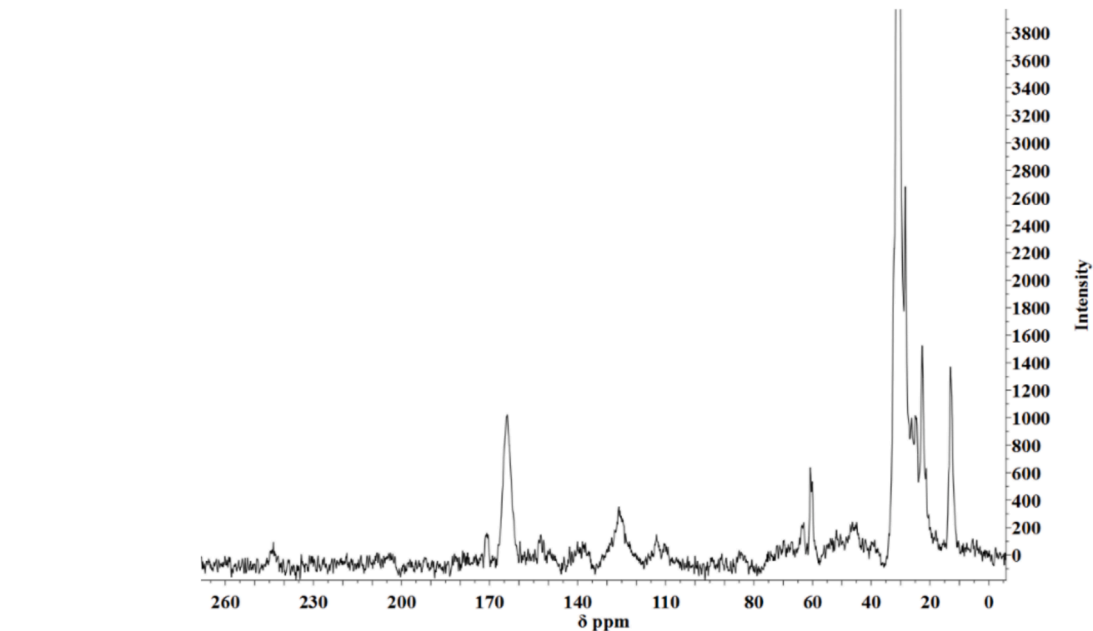


Fig. 4. <sup>13</sup>C CP MAS NMR spectrum of thermochromic pigment.

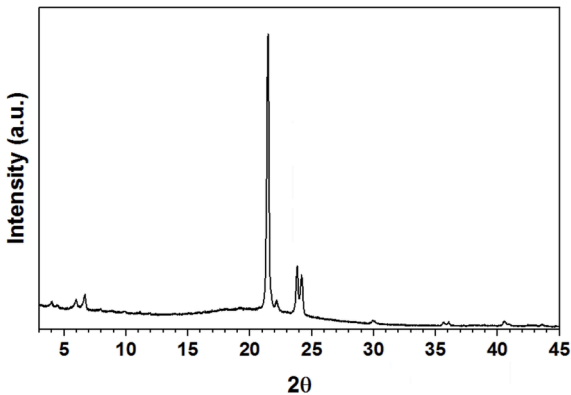


Fig. 5. XRD patterns of photochromic pigment, without baseline correction, scanned at 1.7°/min, from 2θ 3 to 50°, no peaks were detected from 45 to 50°.

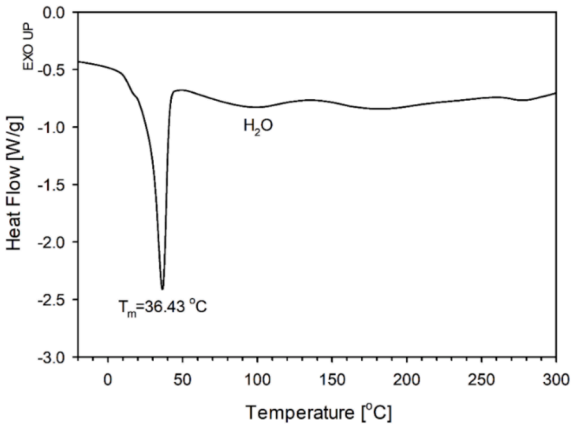




Fig. 6. Differential scanning calorimetry (DSC) thermogram of thermochromic pigment.

**Table 2**  
The colour analysis of the wool sample before and after printing with the paste containing the blue thermochromic pigment. The photographs were taken with an iPhone 13 Pro Max (12 MP sensor, 1.9 μm pixels, 26 mm equivalent f/1.5-aperture lens, sensor-shift OIS, Dual Pixel AF, Apple, Cupertino, CA, USA) at 23 °C in standard D65 light. The measurement error of Lab values is 0.1 %.

Wool sample before printing	Wool sample after printing with the paste containing the blue thermochromic pigment				
					
CIELab analysis					
<i>L</i> <sup>*</sup>	<i>a</i> <sup>*</sup>	<i>b</i> <sup>*</sup>	<i>L</i> <sup>*</sup>	<i>a</i> <sup>*</sup>	<i>b</i> <sup>*</sup>
87.73	−0.10	7.53	57.84	2.92	−47.62

2.2. Elemental analysis





The elemental analysis of the thermochromic pigment was performed with a CHNS analyser model 3018 from EuroVector S.p.A. (Italy). A sample, either analysed or standard, with a weight ranging from 1 to 5 mg and measured with an accuracy of 0.001 mg, was sealed in a tin capsule and loaded into the elemental analyser’s autosampler. The sample was then burnt in an automated process, and the resulting gaseous products were analysed chromatographically.

2.3. X-ray photoelectron spectroscopy (XPS) analysis

The surface atomic composition and chemical states of the thermochromic pigment were measured by X-ray photoelectron spectroscopy (XPS), using a KRATOS AXIS ULTRA spectrometer equipped with a DLD analyser (Kratos-Shimadzu, Kyoto, Japan). The X-ray radiation source was a monochromatic Al Kα (1486.74 eV) with a 120 W X-ray power and an anode voltage of 15.00 kV. The photoexcited electrons were analysed



**Table 3**  
The colour changes of the wool sample with blue thermochromic pigment at various temperatures (15, 23, 30, and 50 °C). The photographs were taken with an iPhone 13 Pro Max (12 MP sensor, 1.9 µm pixels, 26 mm equivalent f/1.5-aperture lens, sensor-shift OIS, Dual Pixel AF, Apple, Cupertino, CA, USA) in standard D65 light. The measurement error of Lab values is 0.1 %.

15 °C			23 °C			30 °C			50 °C		
											
CIELab analysis											
<i>L</i> *	<i>a</i> *	<i>b</i> *	<i>L</i> *	<i>a</i> *	<i>b</i> *	<i>L</i> *	<i>a</i> *	<i>b</i> *	<i>L</i> *	<i>a</i> *	<i>b</i> *
50.18	11.35	−55.98	57.84	2.92	−47.62	88.18	−4.71	−3.26	91.68	−1.83	2.69

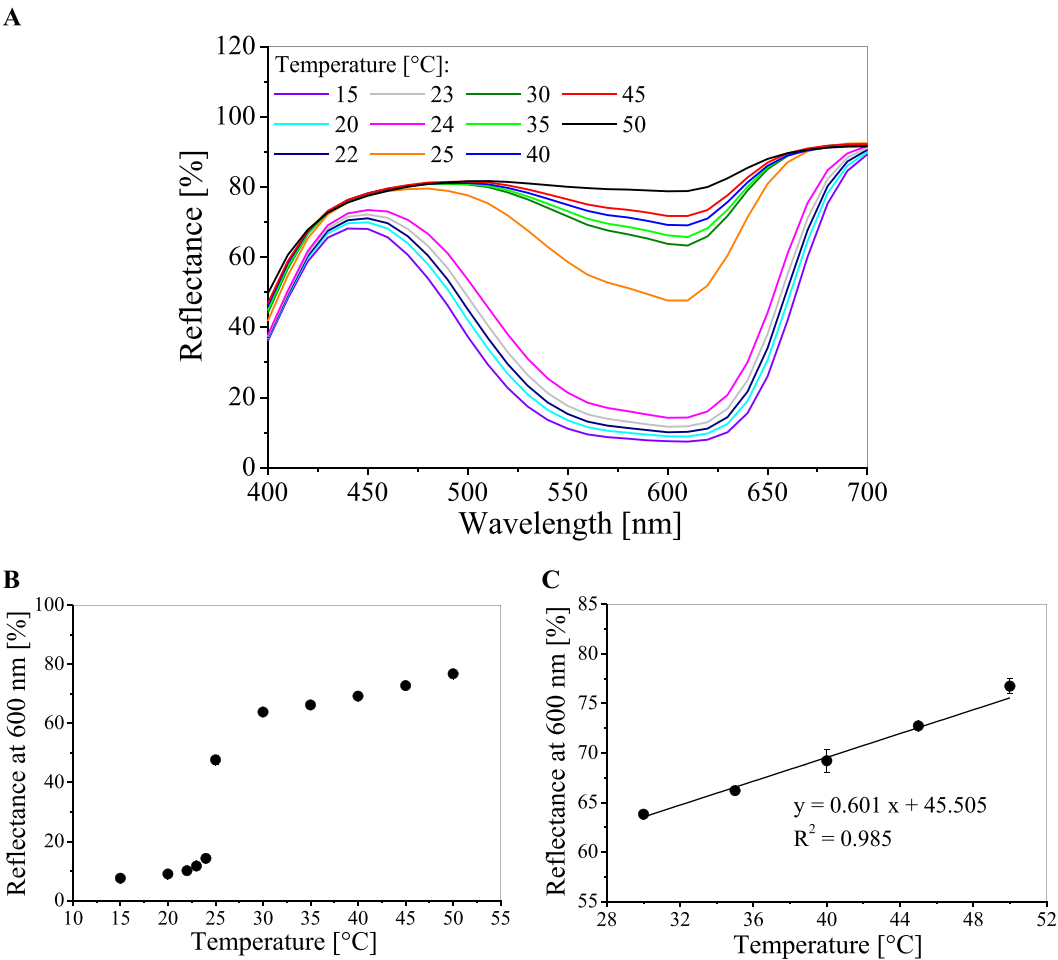


**Fig. 7.** The reflectance spectra of wool fabric printed with a paste containing thermochromic pigment measured at different temperatures in the range of 15–50 °C (A) with the corresponding temperature responses (B, C) and a fitted curve for the linear temperature range (C). Measurements were performed immediately after the sample reached the tested temperature. The results are the average of three measurements.

in constant pass energy mode, using a pass energy of 160 eV for the survey spectra and 20 eV for the high-resolution core level spectra. CasaXPS software was used for data processing.

2.4. Fourier transform infrared spectroscopy (FTIR) analysis

FTIR spectra of the thermochromic pigment were collected at room

temperature on a Nicolet 6700 spectrometer (Thermo Scientific, Waltham, MA, USA) equipped with a deuterated triglycine sulphate (DGTS) detector. The technique of attenuated total refraction (ATR) was used for measurements. The spectra were obtained by adding 128 scans at a resolution of 2 cm<sup>−1</sup>.

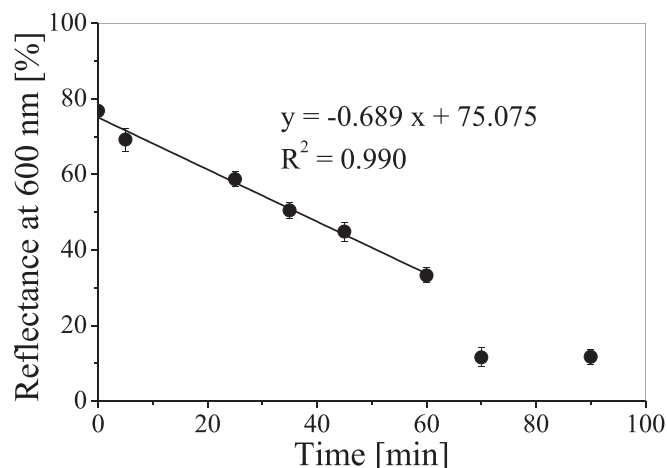


**Fig. 8.** Reflectance values at a selected wavelength (600 nm) of a wool sample printed with a paste with thermochromic pigment, heated to 50 °C, and cooled over time at room temperature (23 °C).

## 2.5. Nuclear magnetic resonance spectroscopy (NMR) analysis

The solid-state  $^{13}\text{C}$  CP MAS NMR spectra were recorded on a Bruker Avance III 400 spectrometer (Bruker BioSpin, Germany) operating at resonance frequencies of 100.627 MHz. In CP MAS experiments, powder samples were packed into a 4 mm  $\text{ZrO}_2$  rotor and spun at a spinning rate of 8 kHz.

## 2.6. X-ray diffraction (XRD) analysis

The crystal structure of the thermochromic pigment was

characterised by X-ray diffraction (XRD) on a PANalytical Empyrean diffractometer with  $\text{Cu K}\alpha$  radiation (Malvern Panalytical, Malvern, United Kingdom). A quick wide  $2\theta$  range scan was performed (5–110°, 9.9 °C/min) as well as a slower scan of the area of interest (3–50°, 1.7 °C/min) to ensure that the structure did not change during the slow scan.

## 2.7. Differential scanning calorimetry (DSC)

Thermal analysis of the thermochromic pigment was conducted by using a DSC TA Q20 analyser (TA Instruments, New Castle, DE, USA). The instrument was calibrated with temperature and heat flow using indium as a standard. The samples (5–6 mg) were weighed accurately into hermetic aluminium pans and pressed slightly to ensure good contact with the DSC cell surface. The data were recorded during heating at a constant rate of 10 °C/min under nitrogen flow with an empty pan as the reference probe.

## 2.8. Preparation of printing paste

In this study, a bleached wool fabric with a 1/1 plain weave (warp: 270/dm, weft: 260/dm, thickness:  $0.38 \pm 0.01$  mm, and a surface mass of  $1.45 \pm 0.02$  g per  $10 \text{ cm}^2$ , Tomtex S.A., Tomaszów Mazowiecki, Poland) was used. This fabric was covered with a printing paste using the screen-printing method. The printing paste contained 15 % w/w acrylic binder Helizarin Binder ET 95 (BASF, Ludwigshafen, Germany), 5 % w/w acrylate-based thickener Lutexal HIT Plus (BASF, Ludwigshafen, Germany), 10 % w/w blue thermochromic pigment TO-NI30 (Chaos Trade, Warsaw, Poland), and 70 % w/w water. The paste was prepared by mixing the binder with the thickener and water and then adding the pigment. All components were weighed using a laboratory balance with an accuracy of  $\pm 0.1$  mg (model: AS220.X2 PLUS, RADWAG, Radom, Poland). The paste was left for 24 h before being used for

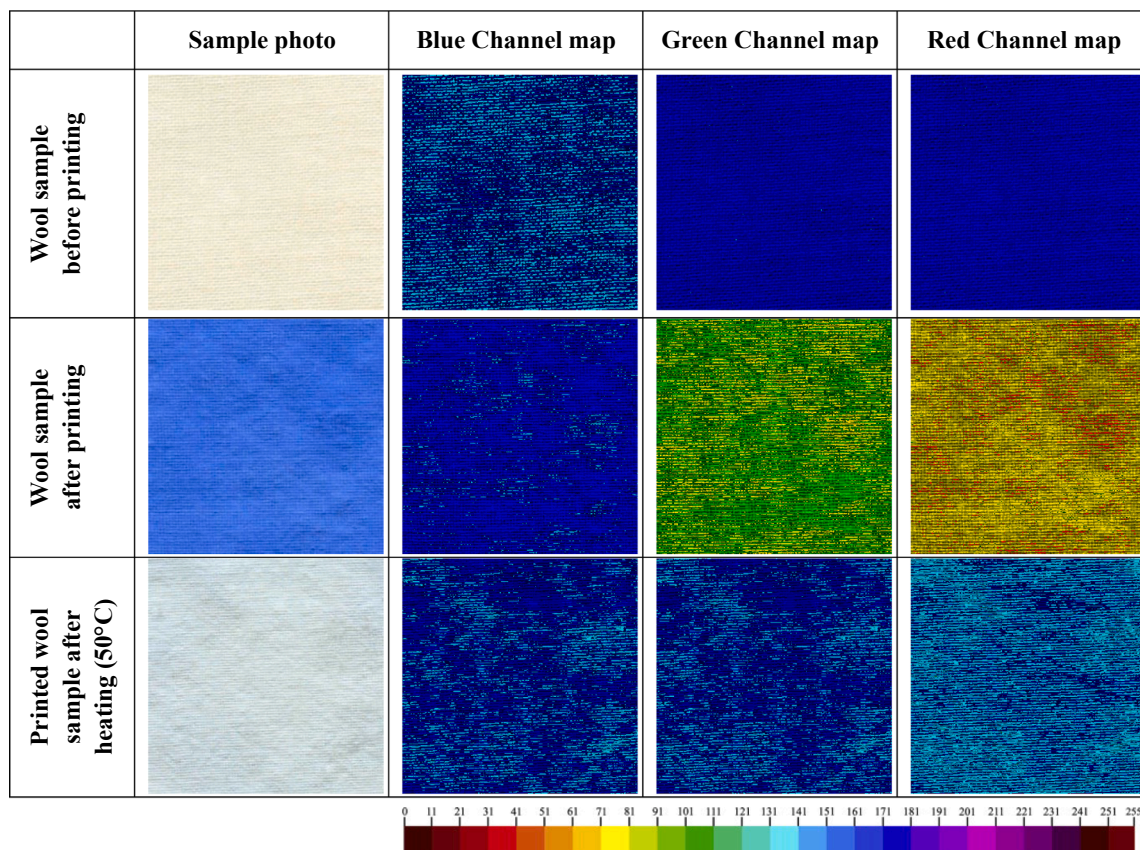


**Fig. 9.** Non-printed wool and wool printed with printing paste containing thermochromic pigment at 23 °C and 50 °C after RGBReader analysis. Colour scale utilised by an algorithm for the analysis of tinge distribution on the surface of textile samples (0: ideal black; 255: ideal white).

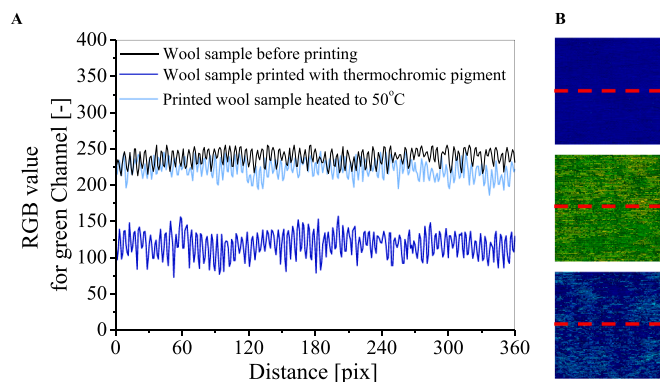


**Fig. 10.** The green RGB channel profiles (1 pix = 0.1 mm) for non-printed, printed with the paste containing thermochromic pigment, as well as printed and heated to 50 °C wool samples (A), together with (B) the images of the RGBReader green channels of samples with red dashed lines to indicate the position of the profiles (from the top: non-printed, printed, printed and heated samples). (For interpretation of the references to colour in this figure legend, the reader is referred to the web version of this article.)

printing. The composition of the printing paste was selected based on recommendations of the manufacturers of individual ingredients.

## 2.9. Screen printing

The printing paste was applied onto the wool fabric by screen printing using a printing screen (EX 63–063/160 PW screen: 63 mesh/cm, thread diameter 63 µm, colour of mesh: white, tension: 18 N/cm, NBC, Tokyo, Japan) and a squeegee. The screens were prepared by covering them with photopolymerisation emulsion and drying at 30 °C for 24 h. Subsequently, foils with the printed designed patterns were placed on the screens and exposed to light (halogen lamp, Halogenfluter 500 W 930037; Düwi GmbH, Breckerfeld, Germany). The light exposure initiated the polymerisation process of the photosensitive emulsion. In areas where the pattern was applied, the polymerisation process did not occur, and the emulsion remained unpolymerised, allowing it to be easily washed away with water. After drying, the screens were used for printing with the printing paste prepared as described in Section 2.8. The paste was spread across the screens using a medium-soft squeegee. Printed wool textiles were dried in a laboratory dryer (model: FD 23, BINDER, Tuttlingen, Germany) at 100 °C for 5 min and then heated at 150 °C for 5 min. For printing,  $0.21 \pm 0.01$  g of the printing paste was used per 10 cm<sup>2</sup> of the wool fabric surface. The A4-sized wool sheets were printed, and samples for each study were cut out from them. For application tests, wool fabric was printed using screens with designed patterns. The patterns were printed with a printing paste containing thermochromic pigment or standard blue pigment (Light blue, BASF, Ludwigshafen, Germany).

## 2.10. Reflectance of light measurements

The reflectance spectra of the printed wool samples were measured with a Spectraflash light reflectance instrument (Spectraflash 300, DataColor, Rotkreuz, Switzerland). The spectrophotometer was equipped with an illuminant D65, and the measurements were registered with a step of 10 nm and a measurement error of 0.1 % at an angle of 10°. The device was calibrated before measurements in accordance with the procedure recommended by the manufacturer. The measurements were performed in the wavelength range of 400–700 nm, with UV light automatically cut off by the software (microMATCH v. 3.6; DataColor, Rotkreuz, Switzerland).

To determine the colour response of the sample as a function of temperature change, the samples were cooled in a refrigerator and heated in a hydraulic press (Blue Press, Schulze, Ravensburg, Germany).

After the sample reached the desired temperature, which was verified with a temperature indicator, it was immediately measured with the spectrophotometer. Based on the spectrophotometric measurements, the colour coordinates were also determined with the CIELab colour system, which describes the perceived colour according to the ISO/CIE 11664–4 standard [25]. Chromatic colours are expressed by the notations  $L^*$ ,  $a^*$ ,  $b^*$ , where “ $L^*$ ” describes the lightness of the colour ranging from 0 (black) to 100 (white), the “ $a^*$ ” determines the colour components on the green–red axis, and the “ $b^*$ ” determines the colour components on the blue–yellow axis. The accuracy of the measurement of colour coordinates in the CIELab system has been investigated and described in a previous paper [26].

## 2.11. Analysis of the surface uniformity of printed textiles

The uniformity of the printed textile surface was analysed. For this purpose, the textile samples measuring  $3 \times 3$  cm<sup>2</sup> were scanned at a resolution of 300 dpi with an Epson Perfection V750 Pro scanner (Nagano, Japan; cold cathode fluorescent lamp; optical resolution Main 6400 DPI  $\times$  Sub 9600 dpi; 48 bit/colour; reflection mode; colour depth 24-bit RGB). Based on the scans, each sample was depicted using a three-colour RGB scale (red, green, and blue), which was conducted with the aid of a script for reading RGB channels (RGBReader; Python Script with Python Imaging Library; DosLab [27]). After preliminary analysis of the test samples, the green channel was selected to create sample profiles because it exhibited the largest changes in values.

## 2.12. Stability tests

The sensors were exposed to UVA radiation ageing (lamp 8 W, type F8T5 Blacklight (range: 315–400 nm; a peak at 369 nm, Hitachi, Japan) in a UVA cabinet (UVP, Upland, Canada). The specified UVA radiation dose was emitted automatically, as the device has a built-in detector with a control system (for example, the emission time of 0.1 J/cm<sup>2</sup> UVA was 57 s). Additionally, changes in reflectance spectra for samples stored for 4 months after their production were examined using a reflectance spectrophotometer (Section 2.10) and compared with the spectra of samples measured immediately after manufacturing.

## 2.13. 2D temperature distribution measurements

Thermochromic sensors were heated or cooled to a selected temperature. The sample temperature was then verified with a temperature indicator, and a photograph of the sample was immediately taken with an iPhone 13 Pro Max. Subsequently, the bitmaps obtained from the captured images were processed using the polyGeVero<sup>®</sup>-CT software package (v.1.2, GeVero Co., Lodz, Poland) and polyGeVero<sup>®</sup> software package (v.2.0, GeVero Co., Lodz, Poland) for further analysis [28]. The software performed image filtering, calibration, and conversion of the obtained results into temperature distribution, illustrated by 2D/3D maps.

## 2.14. Composites preparation

Thermochromic sensors were used as composite elements with a bioepoxy resin matrix (SR GreenPoxy 33 epoxy resin and SD4775 hardener in a weight ratio of 100:27; Sicomin, Châteauneuf-les-Maritiques, France) and reinforcement in the form of a fabric made of wool (weave structure: 1/1 plain, surface weight: 400 g/m<sup>2</sup>, Zakłady Przemysłu Wełnianego TOMTEX S.A., Tomaszów Mazowiecki, Poland), flax (weave structure: 2/2 twill, surface weight: 500 g/m<sup>2</sup>, Libeco, Belgium), glass (weave structure: 1/1 plain, surface weight: 300 g/m<sup>2</sup>, SP-TEX Sp. z o.o., Czechowice-Dziedzice, Poland), or carbon (weave structure: 2/1 twill, surface weight: 280 g/m<sup>2</sup>, SP-TEX Sp. z o.o., Czechowice-Dziedzice, Poland) fibres. The composites were produced by an infusion method.



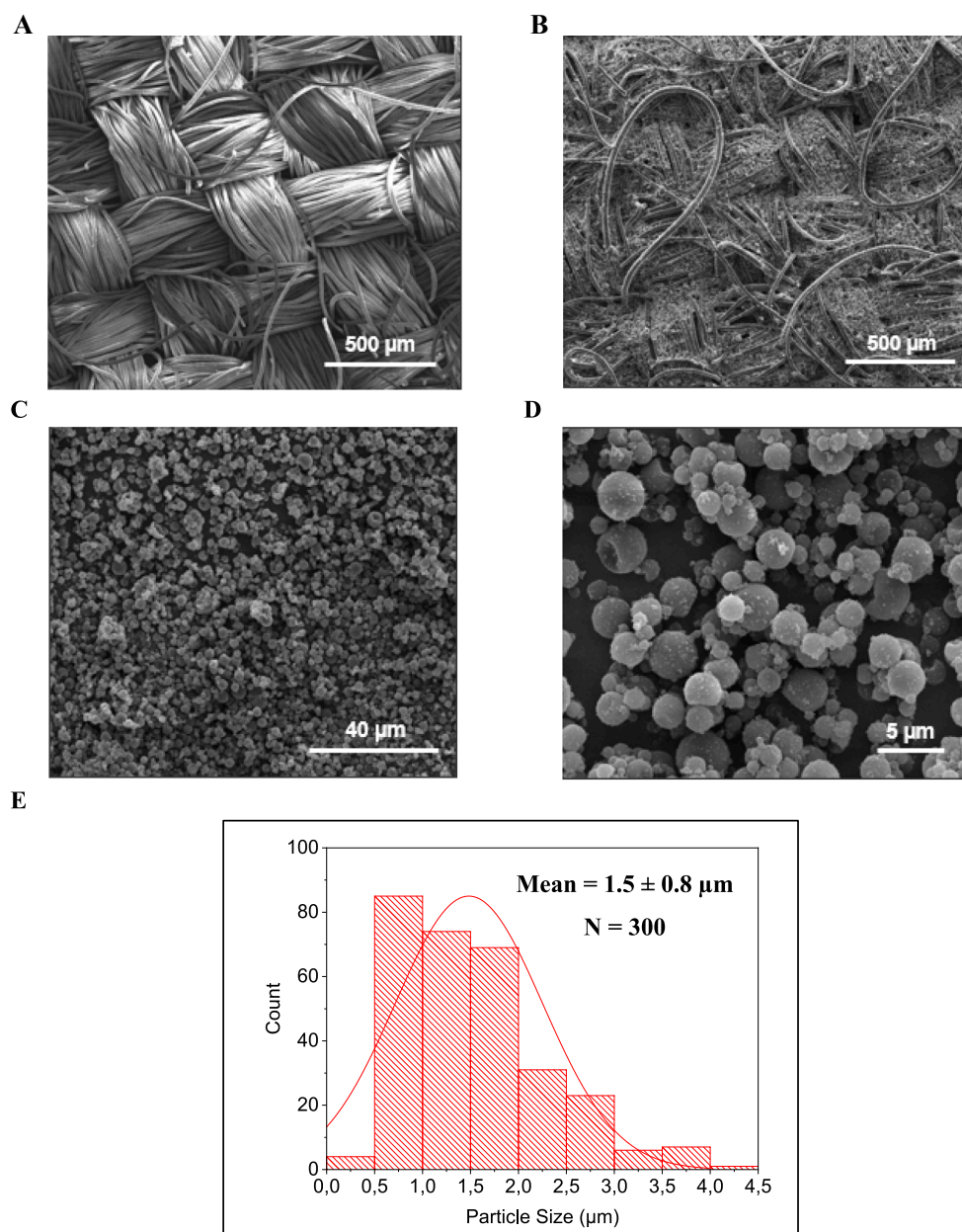


**Fig. 11.** SEM images of non-printed wool at 160× magnification (A), wool printed with printing paste with thermochromic pigment at 160× magnification (B) and 2400× magnification (C), pigment particles at 10000× magnification (D), and the size distribution histogram of the thermochromic pigment particles (E).

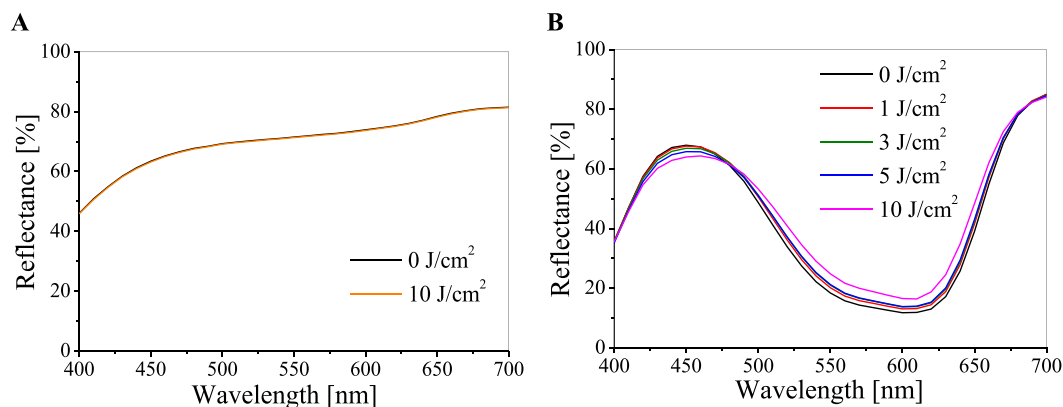
### 3. Results and discussion

#### 3.1. Chemical analysis of thermochromic pigment

A significant challenge lies in accurately determining the origin and chemical composition of commercially available thermochromic colourants. This lack of clarity stems from the frequent omission of complete chemical structure information in manufacturers' product data sheets. Furthermore, literature often incorrectly uses the terms 'dye' and 'pigment' interchangeably when referring to thermochromic compounds, despite their significantly different properties [2,5–10]. However, knowledge of the chemical composition and colourant type is crucial for both basic and application-oriented research involving these compounds. In textile dyeing, the type of colourant directly influences the mechanism of reaction and binding with fibre, and the dyeing techniques used. When dyeing textiles with dyes, selecting a dye with appropriate fibre affinity is essential for establishing permanent fibre-

dye chemical bonds. Dyes are typically applied to dye textiles in dye baths or by printing methods. Pigments, on the other hand, are only used in textile dyeing through printing due to their insolubility in water and common solvents. In this case, a dispersion of pigment in a printing paste consisting of water, thickener, and binder is used. This paste, as a result of the polymerisation process, permanently combines the pigment with the textile material. In this work, an attempt was made to assess the type of colourant used (dye or pigment) and identify its chemical composition using solubility assessment, elemental analysis, as well as EDX, XPS, XRD, FTIR-ATR, NMR, and DSC techniques.

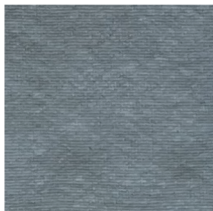

First, a colourant solubility test was carried out using commonly used solvents such as water, acetone, methanol, ethanol, toluene, pyridine, isopropyl alcohol, and dimethylformamide (DMF). For this purpose, 1 mg of the colourant was mixed with 10 ml of pure solvent using a magnetic stirrer (120 min, 250 rpm). In the case of acetone and DMF, the solution was additionally heated to 60 °C. After 7 days from preparation, the solubility of the colourant was assessed organoleptically, and in no



**Fig. 12.** Reflectance spectra of wool samples not irradiated and irradiated with a dose of 10 J/cm<sup>2</sup> UVA (A), and samples of wool printed with a printing paste with a thermochromic pigment, not irradiated and irradiated with doses of 1, 3, 5, and 10 J/cm<sup>2</sup> UVA (B). Measurements were carried out at 23 °C.

**Table 4**

The colour changes of the thermochromic sensor irradiated fractionally and non-fractionally with 100 J/cm<sup>2</sup> of UVA radiation at room temperature (23 °C). The photographs were taken with an iPhone 13 Pro Max (12 MP sensor, 1.9 μm pixels, 26 mm equivalent f/1.5-aperture lens, sensor-shift OIS, Dual Pixel AF, Apple, Cupertino, CA, USA) in standard D65 light. The measurement error of Lab values is 0.1 %.

UVA 100 J/cm <sup>2</sup> given non-fractionally	UVA 100 J/cm <sup>2</sup> given fractionally				
					
<b>CIELab analysis</b>					
<b><i>L</i><sup>*</sup></b>	<b><i>a</i><sup>*</sup></b>	<b><i>b</i><sup>*</sup></b>	<b><i>L</i><sup>*</sup></b>	<b><i>a</i><sup>*</sup></b>	<b><i>b</i><sup>*</sup></b>
66.51	−6.55	−6.32	63.11	−4.39	−33.21

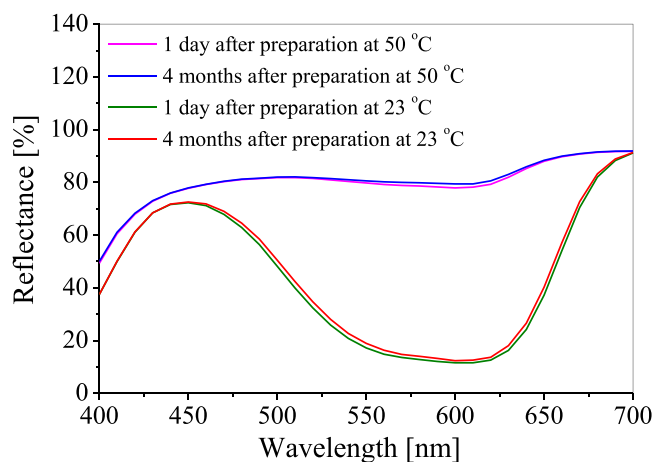


**Fig. 13.** Reflectance spectra of thermochromic sensors 1 day and 4 months after preparation at room temperature (23 °C) and heated to 50 °C.

case was its dissolution observed. Based on this, it can be concluded that the thermochromic colourant used is a pigment.

The data obtained from EDX measurements allowed for the

preliminary determination of the elemental composition on the sample surface. Five analyses were performed on the particles shown in Fig. 1.

This analysis revealed the presence of carbon (63 ± 1 wt%), nitrogen (21 ± 3 wt%), and oxygen (16 ± 2 wt%) (Table 1). The absence of inorganic elements, above the detection limit of the equipment (i.e., around 0.1–0.5 wt%) evidenced the organic composition of the pigment.

Elemental analysis (CHNS), which provides information on precise percentages of mass of individual elements in the entire sample, confirmed the high content of carbon and also indicated the presence of hydrogen and nitrogen in the sample: carbon (C) – 67.81 wt%, hydrogen (H) – 9.69 wt%, nitrogen (N) – 11.12 wt%. Assuming that, in addition to the abovementioned chemical elements, oxygen is also present in the composition of the pigment and its content – determined by subtracting the total percentages of carbon, nitrogen and hydrogen – is 11.38 % wt. Based on the information obtained from the EDX and the CHNS elemental analysis, it can be concluded that the thermochromic pigment is an organic compound containing C, H, N, and O.

The XPS results confirm the presence of carbon, nitrogen, and oxygen on the sample surface (Fig. 2A). Additionally, a small amount of sodium, 0.12 % atomic, was detected. The analysis of the C 1s XPS spectra indicates the presence of carbon in different hybridisations (sp<sup>2</sup> and sp<sup>3</sup>), which is typical for organic compounds with aromatic rings and/or aliphatic chains (Fig. 2B). The peak at approximately 288 eV is assigned to carbon in the N-C=O bond (amide functional group) (Fig. 2B) [29]. Fig. 2C shows the N 1s spectra, the peak at 399.7 eV could be assigned also to the N-C=O bond (amide functional group), and the peak at 398.2 eV corresponds to the R=N-R bond, with R being aromatic (imine functional group) [29,30]. This is in agreement with the fact that in EDX the N/O ratio is higher than 1, indicating that a part of the amide group N is also present in another form. The O 1s spectrum indicates again the presence of an N-C=O bond (amide functional group) (Fig. 2D) [29]. Thus, the XPS analysis has confirmed the presence of aromatic carbons, as well as amide and imine functional groups.

To determine the structural composition of the compound, the elemental composition, FTIR-ATR and NMR analyses were additionally performed. The FTIR spectrum, depicted in Fig. 3, provides insight into the chemical bonding structure of the thermochromic pigment. The absorption band at 3287 cm<sup>-1</sup> corresponds to O-H stretching vibrations, indicating the presence of water in the sample. The peak at 2916 cm<sup>-1</sup> is attributed to the asymmetric C-H stretching vibration of methylene (CH<sub>2</sub>) groups, while the sharp band at approximately 2848 cm<sup>-1</sup> is assigned to the symmetric C-H stretching vibration of methylene groups. An absorption peak around 1730 cm<sup>-1</sup> in an infrared spectrum is attributed to the stretching vibration of the carbonyl (C=O) functional group [31]. Taking into account the conclusions obtained from the XPS analysis, the peak may correspond to the C=O stretching vibration of the amide functional group. The analysed spectrum also exhibits multiple



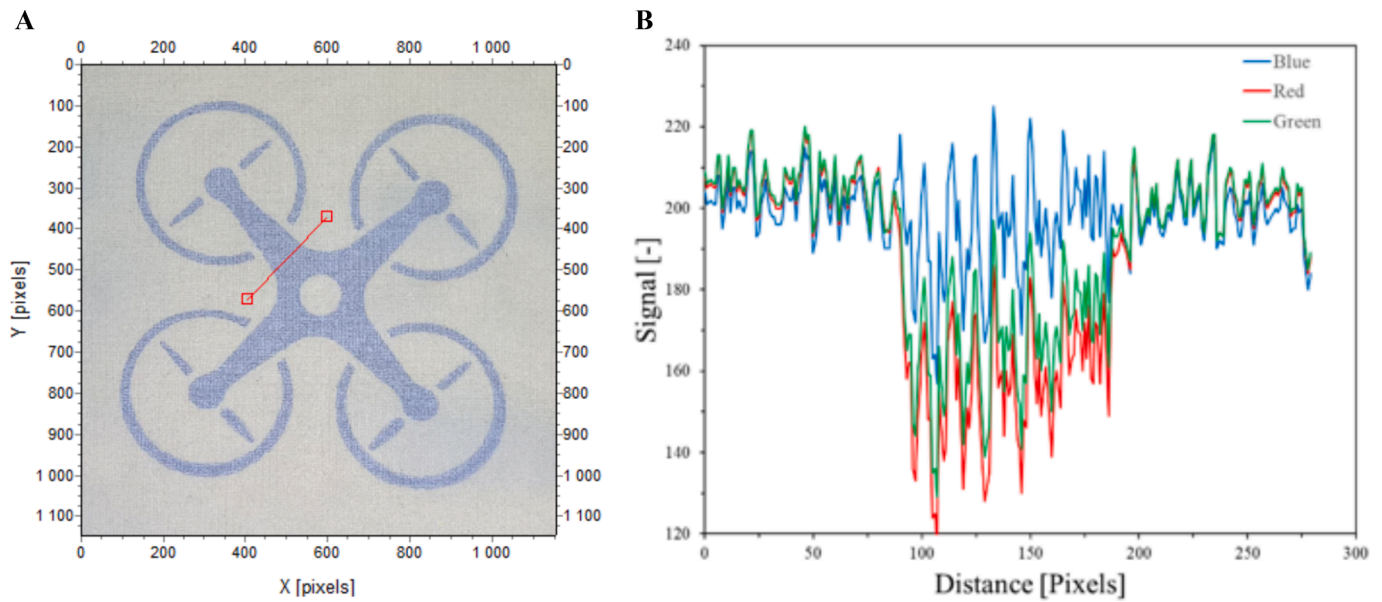


**Fig. 14.** Thermochromic sensor with a marked fragment (red line) (A) resolved into RGB channels (B). (For interpretation of the references to colour in this figure legend, the reader is referred to the web version of this article.)

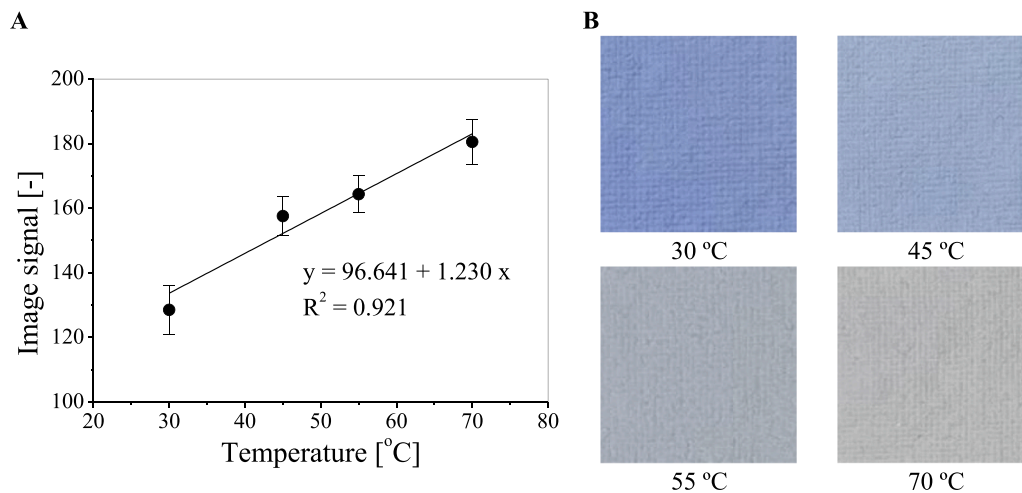


**Fig. 15.** Calibration relation of the red channel values for the RGB colour model depending on temperature (A) with photographs of samples heated to different temperatures, scans of which were used to create it (B). (For interpretation of the references to colour in this figure legend, the reader is referred to the web version of this article.)

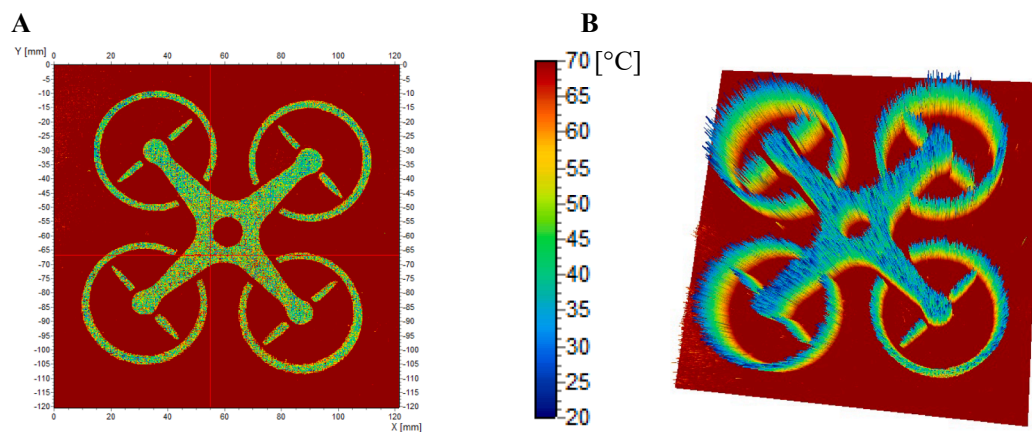


**Fig. 16.** The map of temperature distributions in 2D (A) and 3D using the Plane 3D option of the polyGeVero® software package (B).

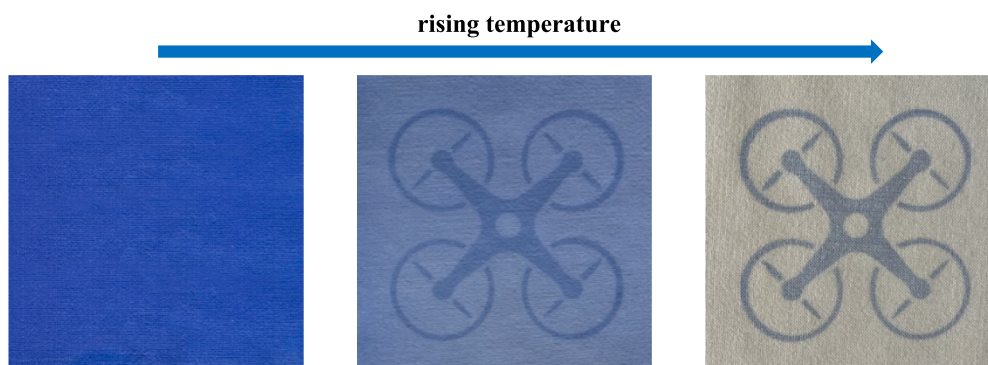


**Fig. 17.** An example of using a thermochromic sensor as a decorative element for a textile product. The decorative pattern (drone) covered with a layer of printing paste with a thermochromic pigment in a darker colour is revealed by heating the sample (temperatures from the left: 23, 30, and 50 °C).

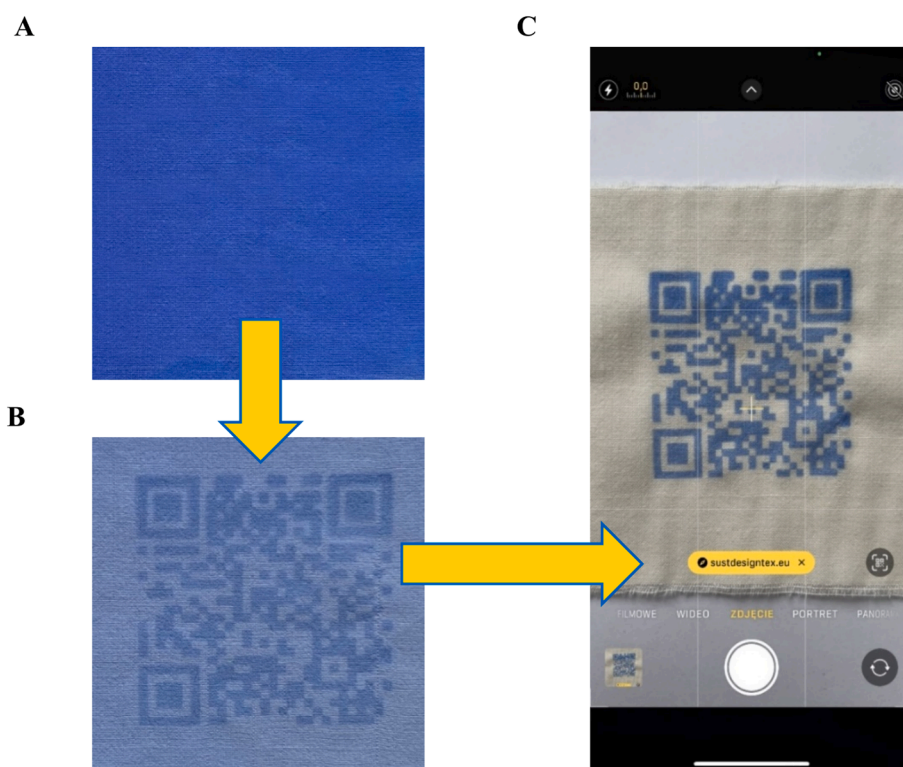


**Fig. 18.** An example of using a thermochromic sensor as a security and marking element for a textile product. A marking pattern (QR code) covered with a layer of printing paste with a thermochromic pigment in a darker colour is revealed by heating the sample from 23 °C (A), through 30 °C (B) to 50 °C (C) until the entire pattern is visible.

peaks indicative of the presence of unsaturated aromatic rings. The absorption bands between 1600 and 1400  $\text{cm}^{-1}$  are associated with C–C stretching vibrations within the ring, whereas the peak at 813  $\text{cm}^{-1}$  suggests benzene ring substitution (aromatic C–H wagging). The wavenumber region 1580–1660  $\text{cm}^{-1}$  is often associated with the N=N and C=N stretching vibration in conjugation with aromatic rings. However, this band can overlap with aromatic C=C stretching vibrations, making it less distinct. At 1347  $\text{cm}^{-1}$ , the FTIR spectrum displays a band associated with C–N stretching vibrations, characteristic of aromatic amines [31,32]. This absorption provides evidence supporting the possible presence of a spirobenzoxadiazine structure within the pigment [33]. Spiro compounds occur in thermochromic pigments, confirming that the compound under investigation is a pigment and not a dye. The absorption at 1013  $\text{cm}^{-1}$  is commonly linked to C–O stretching vibrations in phenolic compounds. The band at 813  $\text{cm}^{-1}$  is often associated with out-of-plane bending (wagging) vibrations of the C–H bonds in an

aromatic ring. This band typically appears in compounds that have substituted benzene rings. The FTIR spectrum also exhibits notable absorption bands at 730  $\text{cm}^{-1}$  and 718  $\text{cm}^{-1}$ , which are typically associated with the out-of-plane bending (wagging) vibrations of aromatic C–H bonds. These bands are characteristic of substituted benzene rings, with the band at 730  $\text{cm}^{-1}$  corresponding to *ortho*-substituted aromatic compounds and the band at 718  $\text{cm}^{-1}$  commonly observed in *meta*-substituted aromatic systems.

The structural analysis of the thermochromic pigment using NMR techniques was greatly hindered due to the pigment's insolubility in known deuterated solvents such as methylene chloride, acetonitrile, acetone, chloroform, benzene, dimethyl sulfoxide, tetrahydrofuran, 1,1,1,3,3,3-hexafluoro-2-propanol, or pyridine. The solid-state  $^{13}\text{C}$  NMR spectrum of the thermochromic pigment is shown in Fig. 4. The spectral pattern confirms that the thermochromic pigment has a spirobenzoxadiazine core structure. According to literature data on solid-

A



B



Fig. 19. Examples of using textile thermochromic sensors as part of clothing (A) and pet accessories (B).

state  $^{13}\text{C}$  NMR, the 10 ppm and 20–25 ppm regions typically correspond to aliphatic methyl and methylene groups [34,35], often attached to the aromatic core or as part of flexible substituents. The signal near 60 ppm can be attributed to methoxy ( $\text{O}-\text{CH}_3$ ) groups or  $\text{C}-\text{N}/\text{O}$  linkages.

The X-ray diffraction was used to investigate the structural characteristics of the thermochromic pigment. The diffractograms obtained during rapid ( $9.9^\circ/\text{min}$ ) (not shown) and slow ( $1.7^\circ/\text{min}$ ) scans revealed the same results, and no damage of the sample was observed in the latter (Fig. 5). The XRD pattern shows a highly crystalline structure characterised by sharp, intense peaks, especially in the range of 20–25 degrees. The absence of significant amorphous scattering further supports the conclusion that the sample is predominantly crystalline. The  $\pi$ -stacking of organic molecules containing aromatic rings gives rise to crystalline diffraction peaks in powders in the region of 18 to  $25^\circ$  revealing intermolecular packing [36]. The main peak at  $21.4^\circ$  corresponds to a  $d$  spacing of 4.2 Å, which is bigger than the 3.4 Å typical to  $\pi$ - $\pi$  intermolecular interactions in graphene, indicating other interactions among the functional groups of the molecules were taking place. A key feature of benzoxadiazine photochromic scaffolds with amide ( $-\text{CONH}-$ ) groups is their ability to form intermolecular hydrogen bonds. An unsubstituted lactam  $\text{N}-\text{H}$  can donate a hydrogen bond to a carbonyl ( $\text{C}=\text{O}$ ) acceptor on a neighbouring molecule. This often leads to robust chains or dimers in the crystal. For example, in some 1,4-benzoxazine (benzoxadiazine) crystal structures,  $\text{N}-\text{H}\cdots\text{O}=\text{C}$  hydrogen bonds link molecules into linear tapes or rings, characterised by single crystal XRD [37]. Such hydrogen-bond networks greatly aid in forming well-organised crystals by anchoring molecules in specific orientations.

Differential scanning calorimetry (DSC) analysis was conducted on the examined pigment to check its thermal properties. Fig. 6 presents the endothermic peaks observed in the first heating curves of the pigment. The DSC thermogram reveals two thermal transitions: water

evaporation from the sample and the melting temperature ( $T_m$ ) of the pigment. The transition associated with water evaporation is relatively broad, with the peak maximum occurring at  $94.73^\circ\text{C}$ , whereas the transition corresponding to the melting of the thermochromic pigment is narrow, with a well-defined peak at  $36.43^\circ\text{C}$ .

### 3.2. Temperature response of thermochromic sensors

The sensors were prepared by applying a blue thermochromic pigment to wool fabric. The screen-printing method with printing paste containing the pigment was chosen for this purpose. Since pigments do not have an affinity for textiles, they are mixed with a printing paste containing a binder, which hardens and polymerises at high temperatures. This process enables the pigment to be effectively fixed onto the surface of the textile substrate [38,39]. The colour of the samples before and after printing was measured using CIELab colour analysis recorded with a reflectance spectrophotometer (Table 2). The thermochromic sensors demonstrate temperature-dependent colour changes. They are blue at room temperature, darken as the temperature decreases, and become lighter as the temperature increases until the sample is completely discoloured at  $50^\circ\text{C}$ . As the temperature increases, the rising value of the “ $L^*$ ” colour coordinate is registered, which represents the increasing lightness of the sample. Simultaneously, a significant increase in the “ $b^*$ ” value is observed, which indicates the disappearance of the blue shade with increasing temperature (Table 3).

The colour change of the sample, depending on temperature, was measured using reflectance spectrophotometry. Samples for measurement were cooled in a refrigerator and heated in a hydraulic press. After cooling or heating, the sample temperature was checked using a temperature indicator, and then the sample was immediately measured using reflectance spectrophotometry. An increase in light reflectance



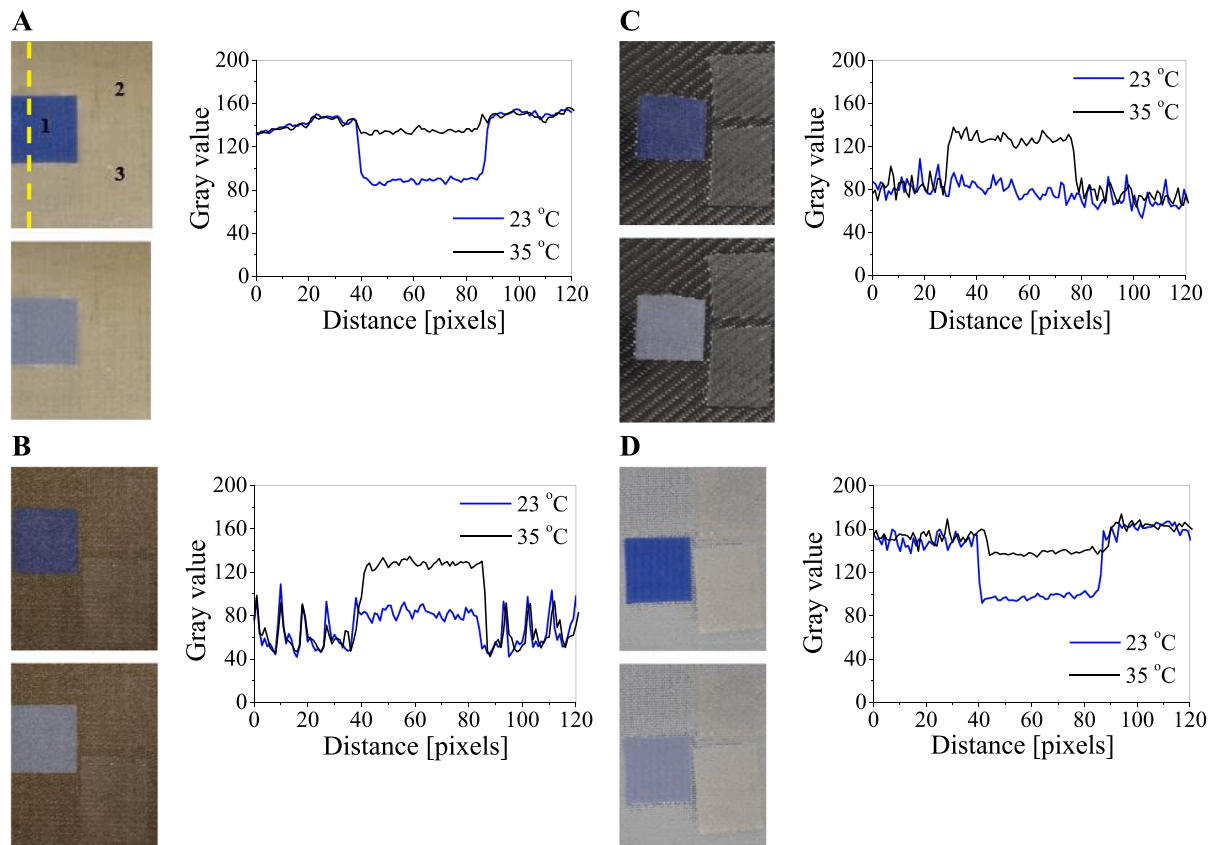


**Fig. 20.** Composites containing (i) bio-epoxy resin, (ii) fabric made of wool (A), flax (B), carbon (C) and glass (D) fibres, and (iii) thermochromic sensor (1). Samples number 2 and 3 are reference samples; 2 is wool covered with printing paste without pigment, and 3 is raw wool. The samples are presented before (top photos) and after heating to 35 °C (bottom photos). The arrangement of the samples is the same in all photos. On the right side of the photos, profiles passing through the samples (in the place marked with a yellow dashed line in A) before (blue) and after (black) heating are presented. The profiles were prepared using the ImageJ software package. (For interpretation of the references to colour in this figure legend, the reader is referred to the web version of this article.)



**Fig. 21.** Examples of using textile thermochromic sensors as part of composites in smartphone (A) and drone (B) casings.

was recorded with increasing sample temperature in the wavelength range from 400 to 700 nm with a minimum at 600 nm (Fig. 7A). This is associated with the occurrence of less and less intense colour until the sample becomes completely discoloured at 50 °C. The beginning of thermal activation of the pigment is observed below 23 °C, and the most significant differences in the reflectance values appear in the range of 30–45 °C, which can be defined as the main range of action of the thermochromic pigment. Based on the reflectance spectra (Fig. 7A), the temperature response of the sensor was plotted, expressed as a reflectance at 600 nm vs. temperature (Fig. 7B). In the temperature range from 30 to 50 °C, a linear increase in the sample reflectance value is observed with increasing temperature (Fig. 7C).

The colour change of the thermochromic sensor presented in this work is reversible, and the rate of return to the original colour depends on the ambient temperature. Fig. 8 presents the changes in the reflectance value of the sample heated to 50 °C for 5 min and then left at room temperature (23 °C). The colour changes, and consequently, the reflectance value changes linearly, up to 60 min after the heating source is removed. The sample returns from the colour it takes at 50 °C (white) to the colour it takes at 23 °C (blue) in 70 min.

### 3.3. The unevenness analysis of the sensor surface

To assess the uniformity of the print, wool samples printed with printing paste with thermochromic pigment were scanned and analysed, describing the RGB (red, green, blue) colour channels. Fig. 9 presents the results for raw wool, samples printed at room temperature, and samples printed and heated to 50 °C. The RGB analysis of the samples revealed a slight unevenness after printing, which is typical of natural fibre fabrics that are not additionally stabilised. However, these irregularities do not affect the overall uniformity of pigment distribution on the fabric surface. The profiles of the raw wool sample and the wool sample printed with a printing paste containing thermochromic pigment at 23 °C and 50 °C were plotted for the green RGB channel (Fig. 10) because the largest changes in the RGB scale values were observed for this channel. The visible unevenness results from the weave of the wool fabric (simple plain weave) and the creases visible on the surface of the material, which are due to the absence of further thermal stabilisation and ironing. Nevertheless, the obtained results indicate high print uniformity of the sample, both at room temperature and after heating to 50 °C.

The morphology of the samples and the uniformity of the print were additionally evaluated using SEM (Fig. 11). The change in the morphology of the sample after printing can be observed. Although the weave structure of the wool fabric remains noticeable, the printing paste with thermochromic pigment forms a uniform layer on the fabric, which indicates good adhesion of the paste to the textile substrate (Fig. 11B). Across the whole printed area, solid spherical particles of the pigment are visible, evenly dispersed in the printing paste on the surface of the wool substrate (Fig. 11C), and in places forming aggregates and agglomerates (Fig. 11C and D). The size distribution of the thermochromic pigment particles is presented in Fig. 11E. Their average diameter is  $1.5 \pm 0.8 \mu\text{m}$ .

### 3.4. Stability tests

Based on organoleptic observations and measurements, it was determined that the primary factor influencing the ageing of thermochromic textile sensors is their exposure to UV radiation. Therefore, ageing tests of the samples were performed by exposing them to UVA radiation in the UV cabinet at doses of 1, 3, 5, and 10 J/cm<sup>2</sup>. UVA radiation was selected for the tests because the samples in the target applications will be exposed mainly to sunlight, which consists of approximately 95 % of UVA radiation [40,41]. The base wool sample showed no changes under the influence of UVA radiation in the range of 0–10 J/cm<sup>2</sup> (Fig. 12A). However, a significant shift in the reflectance spectrum profile of the sample with thermochromic pigment was

observed after exposure to a 10 J/cm<sup>2</sup> dose of UVA radiation (Fig. 12B). The reflectance value at 600 nm then increases by 40.7 %. For lower UVA doses (1, 3 and 5 J/cm<sup>2</sup>), the reflectance increases by 11.1 %, 16.7 %, and 17.4 %, respectively. Despite these changes, all the samples retained their thermochromic properties and continued to respond to temperature variations through colour changes.

The thermochromic sensor becomes destroyed and non-functional when exposed to a high dose of UV radiation. The sensor exhibits significantly greater resistance to the same total dose when it is delivered in smaller, fractional doses than in a continuous dose. For example, Table 4 presents photographs and *Lab* values for a thermochromic sensor exposed to 100 J/cm<sup>2</sup> of UVA radiation continuously and fractionally. The sensor subjected to the full dose in a single exposure was completely destroyed and stopped working. In contrast, the sensor exposed to 100 fractional doses of 1 J/cm<sup>2</sup> retained its thermochromic functionality.

The samples remained stable when stored at room temperature and protected from UV radiation (e.g., covered with aluminium foil). After 120 days of storage, the colour of the samples (reflectance value at 600 nm) changed by 6.7 % at room temperature and by 1.47 % at 50 °C (Fig. 13). These results indicate that it is possible to produce larger batches of samples on a single production line and store them for up to four months before use with almost no impact on the reliability of the temperature reading.

### 3.5. 2D temperature distribution

The possibility of using textile thermochromic sensors to measure the temperature distribution in 2D was tested. For this purpose, a thermochromic sensor in the shape of a drone was prepared. It was heated and cooled to selected temperatures, and at each of them, a photo was taken using an iPhone 13 Pro Max (12 MP sensor, 1.9  $\mu\text{m}$  pixels, 26 mm equivalent f/1.5-aperture lens, sensor-shift OIS, Dual Pixel AF, Apple, Cupertino, CA, USA). All images were processed in the polyGeVero® software. The drone image was decomposed into colour channels in the RGB (red, green, blue) colour model (Fig. 14A). The largest differences in the obtained signal values between the sample at 23 °C (blue) and the sample heated to 70 °C (white) were obtained for the red channel (Fig. 14B) and therefore this channel was selected for further analysis. Images of sensor samples heated and cooled to different temperatures were filtered (settings: kernel size: 3, kernel unit: mm, kernel mode: 2D, iterations: 2) and used to plot the calibration relationship between the values of the red channel of the RGB colour model and the temperature (Fig. 15). Each data point in the chart represents the average value calculated from an image encompassing 7000 to 10,000 pixels of the entire sample. Error bars indicate the standard deviation. As previously noted in the literature [42], the high standard deviation values can be attributed to the inherent noise introduced by the wool fabric's weave structure. To mitigate this issue, a mean filter from the polyGeVero® software package was applied. A linear relationship between the value of the red channel as a function of temperature is observed in the temperature range from 30 to 70 °C (Fig. 15A). Below a temperature threshold of 30 °C, the changes become nonlinear, while above 70 °C, no further alterations are observed due to complete discolouration of the sample.

After calibration, the possibility of measuring the temperature distribution on the sensor surface was checked. For this purpose, a drone pattern was pre-printed on wool fabric using a printing paste with a standard pigment (without thermochromic features) used for printing on textiles. A pigment was added to the paste in such a quantity that its colour corresponded to the colour of a thermochromic printing paste at room temperature. After drying, the entire sample was printed with a printing paste with thermochromic pigment. Then, the sample was placed on a heating plate heated to 70 °C, and discolouration of the thermochromic pigment was observed (background). Photographs were taken using an iPhone 13 Pro Max, scanned, and processed in the polyGeVero® software. Fig. 16 presents a map of the temperature



distribution in 2D (Fig. 16A) and in the 3D plane using the option available in the polyGeVero® software package (Fig. 16B). The obtained results show that the maximum recorded temperature was approximately 70 °C (image background), which is the actual temperature of the heating plate on which the sample was placed. Based on the conducted research, it can be concluded that textile thermochromic sensors can be used to measure the 2D temperature distribution. The flexibility of textile sensors allows for the measurement of temperature distribution on objects of various shapes.

### 3.6. Other application examples

The thermochromic textile sensors presented herein offer a wide range of potential applications. Primarily, they can serve as decorative elements on textile fabrics. It is possible to print various types of patterns using thermochromic pigments, which will change colour under the influence of temperature. It is also feasible to combine underprints made with standard pigments with prints made with thermochromic pigments. The temperature change can then cover or reveal the pattern (Fig. 17). In the same way, thermochromic sensors can be used as protective elements that will be revealed after heating the sample to the appropriate temperature (Fig. 18), thus protecting textile products against counterfeiting. The colour and shade of the underprint can be selected depending on the manufacturer's preferences regarding the temperature limit at which the design is to be revealed.

Moreover, thermochromic sensors can be used as markers on everyday accessories to provide information about the current temperature. Such sensors could be printed on various types of textiles, such as T-shirts, bracelets, hats, headbands, pet leashes, and others, providing high comfort of use (Fig. 19).

The sensors could also be used as elements of composites. This concept was tested by incorporating a sensor in composites composed of a bioepoxy resin matrix reinforced with a fabric made of wool, flax, carbon, or glass fibres. The embedded sensors remained functional, exhibiting colour changes in response to temperature variations, as seen in the photos and profiles presented in Fig. 20. Such composites with thermochromic sensors can be used in various industries where temperature monitoring is necessary, including packaging, electronic components, and the aerospace industry (Fig. 21). A major advantage is that they provide quick and easy-to-read information on the current temperature. It is also possible to select the appropriate pigment depending on the temperature range required in a specific application. Research into sensors as composite elements will be the subject of further studies.

Measurements of colour changes of thermochromic sensors resulting from temperature changes can be performed in the following ways: (i) comparison of the sample colour with a previously prepared colour scale corresponding to the sensor responses at different temperatures, and (ii) measurement of colour using a reflectance spectrophotometer and reading the result from a previously performed calibration relationship. Calibration should be performed individually for each sensor because, depending on storage conditions (e.g., exposure to UV radiation) and application possibilities (used alone or as an element of a composite), the output colour of the sensor at room temperature may vary.

## 4. Conclusions

This article presents the manufacturing process, characterisation, and application potential of thermochromic textile sensors for temperature measurements. These sensors were produced on a wool substrate using a screen-printing technique. The obtained results confirm the uniformity of the print. The developed sensors exhibit a reversible colour change in response to temperature variations, with their colour intensity diminishing as temperature increases until complete discoloration at 50 °C. They demonstrate sustained stability over an extended period (at least four months), however, prolonged exposure to a single dose of high-intensity ultraviolet (UV) radiation (100 J/cm<sup>2</sup>)

leads to a degradation of their functional properties. Furthermore, this paper provides a chemical composition analysis of the thermochromic compound used in the sensor manufacturing process. This analysis determined the thermochromic compound to be an organic pigment with high crystallinity. The structural analysis of the pigment was hindered by its insolubility in common deuterated solvents, but it can be stated that the pigment has a spirobenzoxadiazine core structure with amide (N-C=O) and imine (C=N-C) functional groups.

The new textile thermochromic sensors presented herein offer versatile applications as standalone decorative, marking, informative, and protective indicators, as well as markers for measuring the temperature distribution in 2D. Moreover, they can be integrated as functional components within composite materials. The sensors are characterised by their reversibility and reusability, which can be an advantage or a limitation depending on their intended application. Their production method by single-sided screen printing is simple, rapid, cost-effective, and provides protection against potential skin allergies upon contact. The developed sensors are easy to read, but a certain limitation is the need to prepare a calibration scale or a colour scale for each sensor individually before use. The sensors are flexible, so they can be adapted to a substrate of any shape. Furthermore, it is worth noting that the wool textile used in these sensors is a natural, ecological, and biodegradable material, aligning with the principles of sustainable development.

### Institutional review board statement

Not applicable.

### Informed consent statement

Not applicable.

### CRediT authorship contribution statement

**Malwina Jaszczak-Kuligowska:** Writing – review & editing, Writing – original draft, Visualization, Supervision, Methodology, Investigation, Data curation, Conceptualization. **Elżbieta Sasiadek-Andrzejczak:** Writing – review & editing, Writing – original draft, Visualization, Methodology, Investigation, Data curation, Conceptualization. **Marta Safandowska:** Writing – review & editing, Writing – original draft, Visualization, Methodology, Investigation, Data curation. **Marek Kozicki:** Writing – review & editing, Visualization, Methodology, Investigation, Data curation. **Laura Florentino Madiedo:** Writing – review & editing, Visualization, Methodology, Investigation, Data curation. **Marcin Barburski:** Writing – review & editing, Supervision, Investigation. **David Ranz:** Writing – review & editing, Supervision, Investigation. **Reyes Mallada:** Writing – review & editing, Supervision, Investigation.

### Funding

The research was funded by the Project “Sustainable Industrial Design of Textile Structures for Composites”, funded by the European Union; Grant Agreement no. 101079009 Call: HORIZON-WIDERA-2021-ACCESS-03/Twinning.

### Declaration of competing interest

The authors declare that they have no known competing financial interests or personal relationships that could have appeared to influence the work reported in this paper.

### Acknowledgments

Authors acknowledge the use of instrumentation as well as the technical advice provided by the Spanish National Facility ELECMI ICTS

node “Laboratorio de Microscopías Avanzadas” at the University of Zaragoza.

## Data availability

Data will be made available on request.

## References

- [1] S. Hossain, A. Sadoh, N.M. Ravindra, Principles, properties and preparation of thermochromic materials, *Mater. Sci. Eng.* 7 (2023) 146–156, <https://doi.org/10.15406/mseij.2023.07.00218>.
- [2] P. Kiri, G. Hyett, R. Binions, Solid state thermochromic materials, *Adv. Mater. Lett.* 1 (2010) 86–105, <https://doi.org/10.5185/amlett.2010.8147>.
- [3] M.A. Spirache, P. Marrec, A.J. Dias Parola, C.A. Tonicha Laia, Reversible thermochromic systems based on a new library of flavylum spirolactone leuco dyes, *Dyes Pigments* 214 (2023) 111208, <https://doi.org/10.1016/j.dyepig.2023.111208>.
- [4] A. Hakami, S.S. Srinivasan, P.K. Biswas, A. Krishnegowda, S.L. Wallen, E. K. Stefanakos, Review on thermochromic materials: development, characterization, and applications, *J. Coat. Technol. Res.* 19 (2022) 377–402, <https://doi.org/10.1007/s11998-021-00558-x>.
- [5] A. Gürses, M. Açıkıldız, K. Güneş, M. Sadi Gürses, *Dyes and Pigments*, Springer Briefs in Green Chemistry for Sustainability, Chapter 2: Dyes and Pigments: Their Structure and Properties (2016) 13–29, doi: 10.1007/978-3-319-33892-7\_2.
- [6] R. Rothon, *Pigment and nanopigment dispersion technologies*, Smithers Rapra Publishing, 2012.
- [7] Kirk-Othmer, *Encyclopedia of chemical technology*, fourth edition, Wiley, New York, 1998.
- [8] L. Pereira, M. Alves, Chapter 4: Dyes-environmental impact and remediation, in: A. Malik, E. Grohmann (Eds.), *Environmental Protection Strategies for Sustainable Development, Strategies for Sustainability*, Springer, New York, 2012.
- [9] H. Zollinger, *Colour chemistry: synthesis, properties, and applications of organic dyes and pigments*, Wiley, Zürich Switzerland, 2003.
- [10] Q. Zhang, Q. Nanocolorants, *Handbook of nanophysics: functional nanomaterials*, CRC Press, Taylor & Francis Group, New York, 2010.
- [11] A.B.M. Supian, M.R.M. Asyraf, A. Syamsir, M.I. Najeeb, A. Alhayek, R.N. Al-Dala'ien, G. Manar, A. Atiqah, Thermochromic polymer nanocomposites for the heat detection system: recent progress on properties, *Polymers* 16 (2024) 1545, <https://doi.org/10.3390/polym16111545>.
- [12] H.J. Chen, L.H. Huang, An investigation of the design potential of thermochromic home textiles used with electric heating techniques, *Math. Probl. Eng.* 2015 (2015) 151573, <https://doi.org/10.1155/2015/151573>.
- [13] A. Sadoh, S. Hossain, N.M. Ravindra, Thermochromic polymeric films for applications in active intelligent packaging - an overview, *Micromachines* 12 (2021) 1193, <https://doi.org/10.3390/mi12101193>.
- [14] L. Civan, S. Kurama, A review: preparation of functionalised materials/ smart fabrics that exhibit thermochromic behaviour, *Mater. Sci. Technol.* 37 (2021) 1405–1420, <https://doi.org/10.1080/02670836.2021.2015844>.
- [15] S.M. Nagare, A. Hakami, P.K. Biswas, E.K. Stefanakos, S.S. Srinivasan, A review of thermochromic materials for coating applications: production, protection, and degradation of organic thermochromic materials, *J. Coat. Technol. Res.* (2024), <https://doi.org/10.1007/s11998-024-00982-9>.
- [16] S. Zheng, Y. Xu, Q. Shen, H. Yang, Preparation of thermochromic coatings and their energy saving analysis, *Sol. Energy* 112 (2015) 263–271, <https://doi.org/10.1016/j.solener.2014.09.049>.
- [17] Z. Tatíčková, J. Kudláček, M. Zoubek, J. Kuchar, Behaviour of thermochromic coatings under thermal exposure, *Coatings* 13 (2023) 642, <https://doi.org/10.3390/coatings13030642>.
- [18] H. Liu, Y. Deng, Y. Ye, X. Liu, Reversible thermochromic microcapsules and their applications in anticounterfeiting, *Materials* 16 (2023) 5150, <https://doi.org/10.3390/ma16145150>.
- [19] X. Zhu, Y. Liu, Z. Li, W. Wang, Thermochromic microcapsules with highly transparent shells obtained through in-situ polymerization of urea formaldehyde around thermochromic cores for smart wood coatings, *Sci. Rep.* 8 (2018) 4015, <https://doi.org/10.1038/s41598-018-22445-z>.
- [20] Y. Zhang, Z. Hu, H. Xiang, G. Zhai, M. Zhu, Fabrication of visual textile temperature indicators based on reversible thermochromic fibers, *Dyes Pigm.* 162 (2019) 705–711, <https://doi.org/10.1016/j.dyepig.2018.11.007>.
- [21] W. Zhang, X. Ji, M. Al-Hashimi, C. Wang, L. Fang, Feasible fabrication and textile application of polymer composites featuring dual optical thermoresponses, *Chem. Eng. J.* 419 (2021) 129553, <https://doi.org/10.1016/j.cej.2021.129553>.
- [22] T.A. Elmaaty, S.M. Ramadan, S.M.N. Eldin, G. Elgamel, One step thermochromic pigment printing and Ag NPs antibacterial functional finishing of cotton and cotton/PET fabrics, *Fibers Polym.* 19 (2018) 2317–2323, <https://doi.org/10.1007/s12221-018-8609-x>.
- [23] M. Rožic, N. Šegota, M. Vukoje, R. Kulcar, S. Šego, Description of thermochromic offset prints morphologies depending on printing substrate, *Appl. Sci.* 10 (2020) 8095, <https://doi.org/10.3390/app10228095>.
- [24] M. Vukoje, S. Miljanic, J. Hrenovic, M. Rožic, Thermochromic ink–paper interactions and their role in biodegradation of UV curable prints, *Cellul.* (2018), <https://doi.org/10.1007/s10570-018-970-5>.
- [25] ISO/CIE 11664-4: Colorimetry—Part 4: CIE 1976 L\*a\*b\* Colour Space. CIE Central Bureau: Vienna, Austria, 2019.
- [26] M. Jaszczak-Kuligowska, E. Szaidek-Andrzejczak, M. Kozicki, Elastic TTC–PVA gel dosimeters for personal UV exposure measurements, *Measurement* 228 (2024) 114332, <https://doi.org/10.1016/j.measurement.2024.114332>.
- [27] M. Kozicki, E. Szaidek, Scanning of flat textile-based radiation dosimeters: Influence of parameters on the quality of results, *Radiat. Meas.* 58 (2013) 87–93, <https://doi.org/10.1016/j.radmeas.2013.08.011>.
- [28] M. Kozicki, P. Maras, A.C. Karwowski, Software for 3D radiotherapy dosimetry, *Validation Phys. Med. Biol.* 59 (2014) 4111–4136, <https://doi.org/10.1088/0031-9155/59/15/4111>.
- [29] G. Beamson, D. Briggs, *High resolution XPS of organic polymers - the scienta ESCA300 database*, Wiley Interscience, 1992.
- [30] C. D. Wagner, A. V. Naumkin, A. Kraut-Vass, J. W. Allison, C. J. Powell, J. R. Jr. Rumble, NIST Standard Reference Database 20, Version 3.4, web version: <http://srdata.nist.gov/xps/> (2003).
- [31] B.C. Smith, *Infrared spectral interpretation, a systematic approach*, Boca Raton, Imprint CRC Press, 1999, 10.1201/9780203750841.
- [32] F.B. De Sousa, J.D.T. Guerreiro, M. Ma, D.G. Anderson, C.L. Drum, R.D. Sinisterra, R. Langer, Photo-response behavior of electrospun nanofibers based on spiropyran-cyclodextrin modified polymer, *J. Mater. Chem.* 20 (2010) 9910–9917, <https://doi.org/10.1039/C0JM01903H>.
- [33] J.-L. Wang, R. Zhao, J.-L. Dai, P.-K. Jia, B.-W. Yin, H.-G. Wang, B.-B. Xie, A different photochromic mechanism of spirooxadiazine: electronic structure calculations and nonadiabatic dynamics simulations, *Dyes Pigm.* 230 (2024) 112332, <https://doi.org/10.1016/j.dyepig.2024.112332>.
- [34] M.J. Simpson, A.J. Simpson, W.L. Kingery, Solid-state <sup>13</sup>C nuclear magnetic resonance (NMR) analysis of soil organic matter, *Ref. Module Earth Syst. Environ. Sci.* (2017), <https://doi.org/10.1016/B978-0-12-409548-9.10275-1>.
- [35] H. Günther, *NMR Spectroscopy: Basic Principles, Concepts and Applications in Chemistry*, Wiley-VCH, 2013.
- [36] M. Tang, S. Zhu, Z. Liu, et al., Tailoring  $\pi$ -conjugated systems: from  $\pi$ - $\pi$  stacking to high-rate-performance organic cathodes, *Chemistry* 4 (2018) 2600–2614, <https://doi.org/10.1016/j.chempr.2018.08.014>.
- [37] I.V. Ozhogin, V.V. Tkachev, B.S. Lukyanov, et al., Synthesis, structure and photochromic properties of novel highly functionalized spiropyran of 1,3-benzoxazin-4-one series, *J. Mol. Struct.* 1161 (2018) 18–25, <https://doi.org/10.1016/j.molstruc.2018.02.027>.
- [38] A. Dessie, B. Eshetu, *The role of binders and its chemistry in textile pigment printing*, *J. Textile Sci. Eng.* 11 (2021) 428.
- [39] R.M. Christie, *The Chemistry of Color Application*, Blackwell Science, England, 2000.
- [40] J. D’Orazio, S. Jarrett, A. Amaro-Ortiz, T. Scott, UV Radiation and the Skin, *Int. J. Mol. Sci.* 14 (2013) 12222–12248, <https://doi.org/10.3390/ijms140612222>.
- [41] IARC Working Group Reports, Exposure to artificial UV radiation and skin cancer, World Health Organization, France (2005).
- [42] M. Kozicki, E. Szaidek, Scanning of flat textile-based radiation dosimeters: influence of parameters on quality of results, *Radiat. Meas.* 58 (2013) 87–93, <https://doi.org/10.1016/j.radmeas.2013.08.011>.